

Numerical Simulation of the Store Separation Using Unstructured Cartesian Grid*

Weimin Sang¹, Fengwei Li², and Qin E³

Department of Aircraft Engineering, Northwestern Polytechnical University
Xi'an, 710072, People's Republic of China

Keywords: unstructured Cartesian grid, tree data structure, store separation

Abstract

A new unstructured Cartesian grid generation method is presented. The grid generation of some airfoils and wing is performed with the tree data structure. Euler equations are solved using the cell-centred finite volume method. The results of flow field computation are in good agreement with the experiments. These facts show that the grid generation and the numerical calculation approach are correct and reasonable.

Based on the above work, a flow field numerical simulation of wing and store separation is finished. This process provides a new way and tool for the more accurate solver of the unsteady flow problem.

Introduction

In the CFD development, there is an urgent requirement for the accurate and efficient grid generation method to the complex configuration in reality. So many grid generation methods have greatly improvement and very quick development. Recently, there has been a

renewed most interest in using unstructured Cartesian grid. For very complex configuration, coupled with tree data structure and grid adaptation, the grid method has been demonstrated to be very viable and efficient tool.

In the work presented in this paper, Euler equations are solved using the above grids and the cell-centred finite volume method. Many test cases are finished, including NACA0012 and RAE2822 and GAW-1 and three-element airfoils and ONERA M6 wing. The good agreement between computational results and experimental data shows the flexibility and accuracy of the approach.

The stores of the advanced aircraft are increasing. The security and flight control of the store has already become one of major problems for the people. In course of the aircraft devise, the store carriage is one of the important considered factors. The experiments of the store separation need higher cost and longer time, and maybe very difficult for offering the full and exact data. But, the CFD developments supply a new

* Supported by the Doctorate Foundation of Northwestern Polytechnical University.

¹ Candidate for Doctor Degree, Department of Aircraft Engineering, P.O.Box 114.

² Prof. Dr.-Ing., Department of Aircraft Engineering, P.O.Box 114, Member AIAA.

³ Professor, Department of Aircraft Engineering, P.O.Box 114.

approach for studying the store separation problem. The new method may decrease experiment time and reduce the research cost.

In this paper, the unsteady flow case is solved, which is separation of wing and ellipsoid store. The computation includes two steps. Firstly, the unsteady Euler equation is solved by the use of the Cartesian grid approach. From the above computation, the aerodynamics can be given in every time step. Secondly, movement track of the store is performed with the rigid-body dynamics movement equations. At the same time, the grids are modified by the Cartesian grid methodology. The numerical results prove that the grid generation method is very efficient and correct.

1. Unstructured Cartesian grid

In the recent years, the unstructured Cartesian grid method [1,3] has a very quick development and improvement due to continued difficulties with body-fitted grid generation. So, there has been a great interest in using the Cartesian grids. The methods have been demonstrated to be very viable tools for inviscid flows, with very complex geometry.

The main advantages of the Cartesian grid method are the following:

1. easy grid generation
2. automatic grid adaptation
3. simplified data structure

One of the most appealing properties of the Cartesian grids is its efficiency in filling space with a minimum number of cells and faces given a certain grid resolution. Of course, there is one reason to prefer the Cartesian grid method. It allows the use of higher order accurate shock capturing methods that are difficult to achieve on the other grids.

The Cartesian grid method uses a non-body-fitted grid of rectangular cells to discretize the flow field about an object [2,4]. The grid cells are generated from one large root cell, which covers the complete flow field through recursive the Quadtree (2D) or the Octree (3D) subdivisions. The root cell is subdivided recursively until a given specified minimum grid resolution is obtained. After creating this surrounding mesh of rectangular cells, the surface geometry is simply “cut out” from the underlying cells, leaving a border of irregular cells surrounding the object. The method has the potential to greatly simplify and automate the difficult task of grid generation around complex configuration.

In the end, Cartesian grid cells are cut the following parts, Wall Cells and Solid Cells and Flow Cells. Wall Cells is cells which are intersected by the body surface, and cells that are located inside the body surface are named Solid Cells, and the rest of the cells are called Flow Cells. In the Wall Cells, small cells exist, which could induce the instability and bad convergence of the flow field. So, the small cells should be combined with its the near cell which is suitability to itself.

In the above Cartesian grid, the use of tree data structure quicken rate of grid generation, and take easiness the search of grids relation, and reduce greatly time of grids generation. For grid generation and flow computation in this paper, data management uses a new style, which data are divided three classes of grid and face and point. The new style is very useful to write the program code of grid generation and flow computation. For example, faces have the direction attribute, x or y or z direction for 3D. At the same time, faces are given the serial

number of grid, which lies to two sides of the face. So flux computation of flow become very fast.

2. Flow computation

According to the conservation principle for mass, momentum and energy, in a three-dimensional domain of volume Ω with boundary S , the unsteady Euler equations may be written in the following integral form

$$\frac{\partial}{\partial t} \int_{\Omega} W d\Omega + \int_S \vec{F} \cdot \vec{n} ds = 0$$

where W is the vector of conserved variables, and \vec{F} is the flux vectors

$$W = \begin{pmatrix} \rho \\ \rho u \\ \rho v \\ \rho w \\ \rho E \end{pmatrix}$$

$$\vec{F} = \begin{pmatrix} \rho u & \rho v & \rho w \\ \rho u^2 + p & \rho v u & \rho w u \\ \rho u v & \rho v^2 + p & \rho w v \\ \rho u w & \rho v w & \rho w^2 + p \\ \rho u H & \rho v H & \rho w H \end{pmatrix}$$

E and H are the total energy and total enthalpy respectively. These quantities are related to each other by the definitions of total energy and total enthalpy per unit volume. For a perfect gas

$$\rho E = p / (\gamma - 1) + \rho (u^2 + v^2) / 2$$

$$\rho H = \rho E + p$$

Performing the spatial discretization, the integral form of Euler equations for a cell i can be written as

$$\frac{dW_i}{dt} = - \frac{\int_{S_i} \vec{F} \cdot \vec{n} ds}{\int_{\Omega_i} d\Omega}$$

Next, the equation leads to the ordinary differential equations with respect to

time

$$\frac{d}{dt} W + R = 0 \quad R = \frac{1}{V} Q$$

where R is the residual, V is the volume of the cell, and Q is a discrete approximation of the flux integral.

For the above ordinary differential equations, the Runge-Kutta stepping scheme can be employed here. In the present work, the equation is performed with an explicit 4-stage scheme.

Cell central scheme such as the one described above are non-dissipative, so that even and odd point oscillations may be presented in the steady-state solution. In order to eliminate these oscillations, artificial dissipative terms are added to the residual

$$R = \frac{1}{V} (Q - \bar{D})$$

where \bar{D} is the dissipation function, which is constructed as a blending of second and fourth differences of the conserved variables in Ref. 5.

Convergence to the steady-state solution can be accelerated using several common techniques, and those implemented in the present method involve the use of a local time step, together with enthalpy damping and implicit residual smoothing.

3. Separation and fall of the store

3.1. flow computation of separation and fall

The numerical simulation of this unsteady problem is very complex and difficult, because of using the alterable boundary condition of wall surface and the minimum time step in the whole flow field. In order to solve the question, people try to employ the overlapped structure grids and the unstructured grid methodology of movable pulling and

extending. Having good automatic generation characteristic, but the pulling and extending of unstructured grids could bring very greatly grids aberration. For the overlapped grids system, wing and store can be generated the very good body-fitted grids, but interpolation calculation of flow information transformation among grids could take a lot of trouble.

For flow field computations of separation and fall, Cartesian grids have more peculiarity, and no have very costly interpolation calculation of the overlapped grids, and no have unstructured grids pulling and extending aberration. Cartesian grids need only the new cutting in the new falling position. The unsteady problem can be solved easily by use of the Cartesian grids.

3.2. computation of fall track

From the knowledge of theory mechanical, the commonly movement of rigid-body can be decomposed two parts, which are plane movement and fixed-point rotation movement.

The computational method of fall track is developed which couples with the rigid-body dynamics equations in six degrees of freedom. The equations can be expressed as follows:

$$\vec{s} = \vec{v}_0 t + \frac{1}{2} \vec{a} t^2$$

$$\vec{\theta} = \vec{\omega}_0 t + \frac{1}{2} \vec{\varepsilon} t^2$$

4. Test cases and conclusions

The main purpose of the test cases is to demonstrate the validity and capability of the above grid generation and flow solver. Some 2D and 3D test cases are presented in this paper.

4.1. Flow around some airfoils

(1) flow around NACA 0012 airfoil

The flow initial conditions are $\alpha = 0.0^\circ$, $\alpha = 2.0^\circ$ and $M = 0.77$. The grid is displayed

in Fig.1. It is obvious that refined grid cells were automatically generated for leading and trailing edges of the airfoil. The computed pressure coefficient profile at airfoil surface is compared with experimental data in Fig.3.

(2) flow around RAE 2822 airfoil

In Fig.2, The computational grid is shown. The flow initial condition is $\alpha = 3.19^\circ$ and $M = 0.75$. Same as the test (1), the refined grid cells can be automatically generated for leading and trailing edges of the airfoil. The computed pressure coefficient profile at airfoil surface is compared with experimental data in Fig.4.

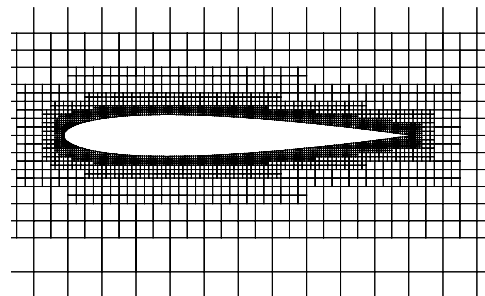


Fig.1. NACA 0012 Airfoil, Grid

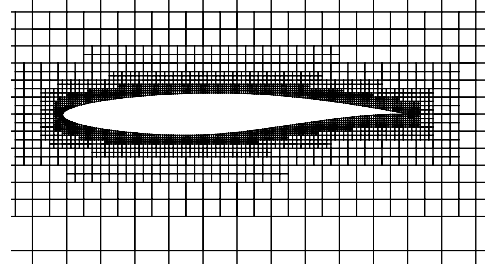


Fig.2. RAE 2822 Airfoil, Grid

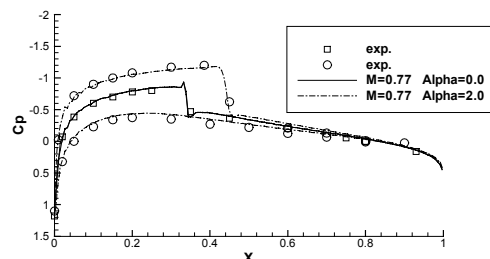


Fig.3. NACA 0012 Airfoil, Cp on Surface

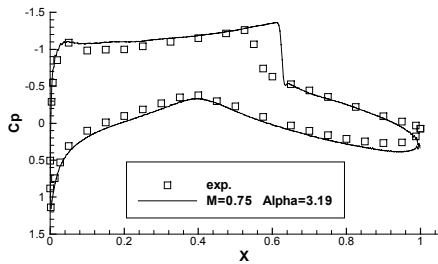


Fig.4. RAE 2822 Airfoil, Cp on Surface

(3) flow around GAW-1 airfoil

This is a two-element airfoil. The flow initial condition is $\alpha = 10.3^\circ$ and $M = 0.13$. The computational grid is displayed in Fig.5. It is obvious that refined grid cells were automatically generated for leading and trailing edges of the two-element airfoil. The computed pressure coefficient profiles and experimental data at airfoil surface are shown in Fig.6.

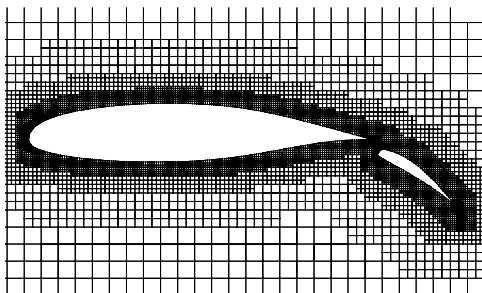


Fig.5. GAW-1 Airfoil, Grid

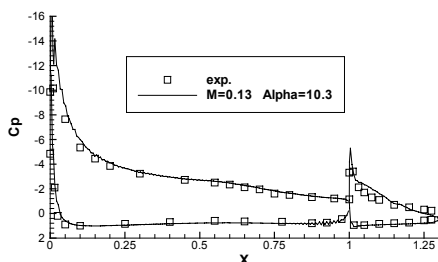


Fig.6. GAW-1 Airfoil, Cp on Surface

(4) flow around three-element airfoil

The flow initial condition is $\alpha = 0.0^\circ$ and $M = 0.2$. The computational grid is shown in Fig.7. The computed pressure coefficient profiles and

experimental data at airfoil surface are compared in Fig.8. The capability of the current approach for complex configuration is demonstrated.

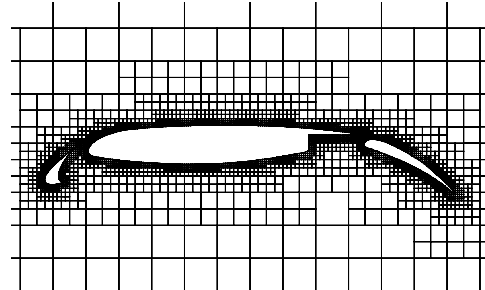


Fig.7. Three-element Airfoil, Grid

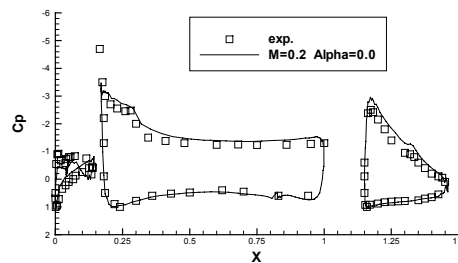


Fig.8. Three-element Airfoil, Cp on Surface

4.2. Transonic flow around ONERA M6 wing

The flow initial conditions are $\alpha = 3.06^\circ$ and $M = 0.8399$. The wing computational grid is displayed in Fig.9. It is obvious that refined grid cells were automatically generated for wing leading and trailing edges and wing tip. In Fig.10, the contours of Mach number are shown. The computed pressure coefficient profile at wing surface is compared with experimental data at four span-wise sections in Fig.11 (a) – (d). It is observed that good agreement was obtained as a whole. In order to display clearly grid details in the flow space, some grid section figures is shown in Fig.12.

The above flow computation results prove that grid generation and flow

solver are correct and capability. At the same time, the Cartesian grid method has been demonstrated to be very viable and efficient.

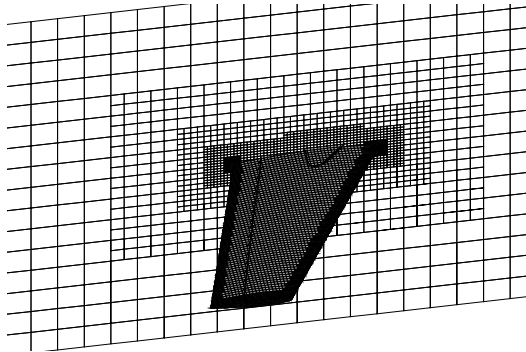


Fig.9. ONERA M6 Wing, Grid

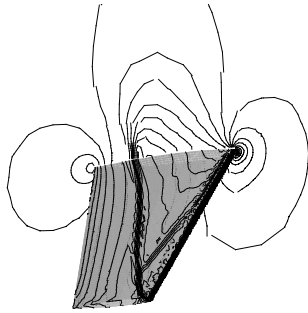
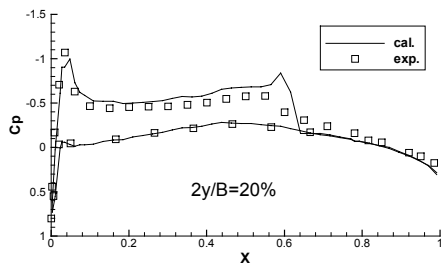
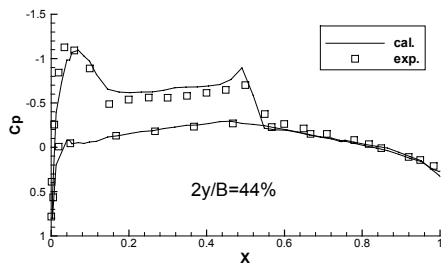


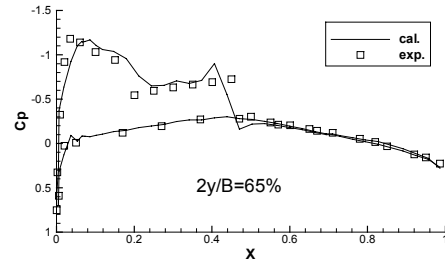
Fig.10. M6 Wing, Mach Number Contours



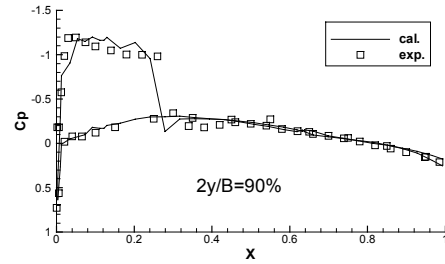
(a)



(b)



(c)



(d)

Fig.11. ONERA M6 Wing, Cp at Different Spanwise Stations ($M_\infty = 0.8399$, $\alpha = 3.06^\circ$)

4.3. Flow of the ONERA M6 wing and store separation and fall

The store is an ellipsoid volume, which long and short axis ratio is 3.0. In the flow movement, the wing is stillness relatively. The initial flow conditions are $\alpha = 3.0^\circ$ and $M = 0.4$. The flow system is at high air of 2000 meters. The wing computational grid is displayed in Fig.13. To reduce the grid number and computation time, fine grid cells were automatically generated only for wing leading edges. In Fig.14 (a) and (b), the computed fall track is presented from the different direction.

The preliminary results indicate that the unsteady CFD algorithm, dynamic grid technique, and the rigid-body-dynamics algorithm work well in concert to produce the unsteady solution of a complex, and three-dimensional problem involving relative body motion.

The present approach can be extended to some new applications in numerical simulation of the store separation.

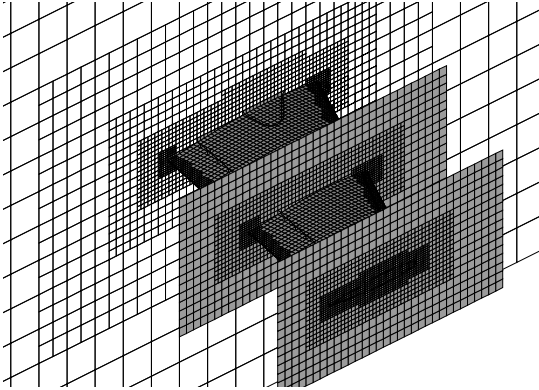


Fig.12. ONERA M6 Wing, Grid(Detail)

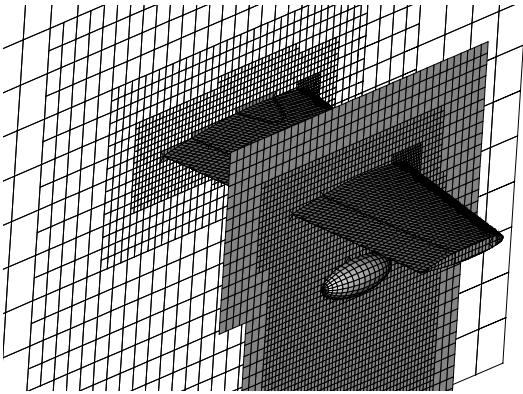
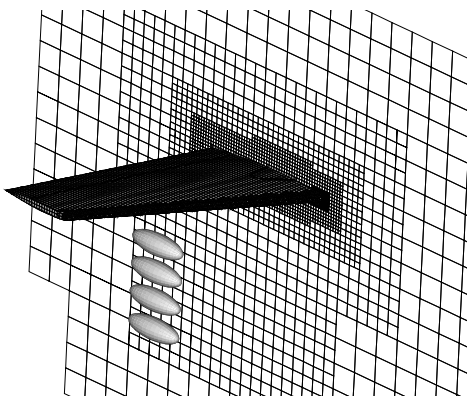
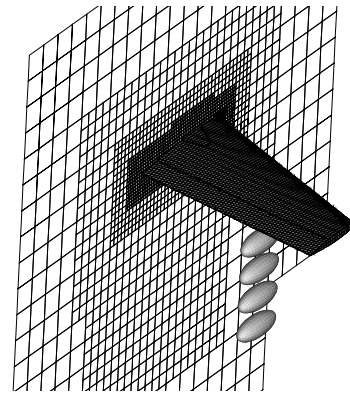


Fig.13. Separation of Wing and Store, Grid(Detail)



(a) Front View



(b) Rear View

Fig.14. Separation of Wing and Store, Computed Fall Track

The ultimate goal of the present research is to produce a useful, commercially viable CFD tool to solve real life flow problems. This work is now underway.

References

- [1] Wang,Z.J., Chen,R.F., N.Hariharan and A.J.Przekwas, "A 2nd Tree Based Automated Viscous Cartesian Grid Methodology for Feature Capturing", AIAA-99-3300, 1999
- [2] Karman, S.L., "SPLITFLOW: A 3D unstructured Cartesian/Prismatic Grid CFD Code for Complete Geometries", AIAA-95-0343, 1995
- [3] Wang,Z.J., "Proof of Concept – An Automatic CFD Computing Environment with a Cartesian Prism Grid Generator, Grid Adaptor and Flow Solver", in Proceeding of 4th International Meshing Roundtable, pp87-99, October 1995, Albuquerque, New Mexico
- [4] John E. Melton, Marsha J. Berger, Michael J. Aftosmis, Michael D. Wong, "3D Application of a Cartesian Grid Euler Method", AIAA 95-0853, 1995
- [5] Aparajit.J.Mahaian, Eari.H.Dowell, Donald.B.Bliss, "Role of Artificial Viscosity in Euler and Navier-Stokes Solvers", AIAA Journal Vol. 29, No. 4, April 1991